

NOTAS DE FÍSICA

VOLUME XIX

Nº 14

STUDY OF THE ELECTRIC QUADRUPOLE INTERACTION (EQI) IN
 $(\text{Pb}_{0.925} - \text{Ba}_{0.075})\text{ZrO}_3$ BY PERTURBED
ANGULAR CORRELATIONS

by

Henrique Saitovitch

and

Joachim Bernd Fechner

CENTRO BRASILEIRO DE PESQUISAS FÍSICAS
Av. Wenceslau Braz, 71 - Botafogo - ZC-82
RIO DE JANEIRO, BRASIL
1973

STUDY OF THE ELECTRIC QUADRUPOLE INTERACTION (EQI) IN $(\text{Pb}_{0.925}\text{-Ba}_{0.075})\text{ZrO}_3$
BY PERTURBED ANGULAR CORRELATIONS

Henrique Saitovitch

*Centro Brasileiro de Pesquisas Físicas
Rio de Janeiro, Brazil*

and

Joachim Bernd Fechner

*Institut Für Strahlen und Kernphysik der Universität Bonn
Bonn, Germany*

(Received 16th May 1973)

ABSTRACT

The EQI in polycrystalline $(\text{Pb}_{0.925}\text{-Ba}_{0.075})\text{ZrO}_3$ has been investigated in the temperature range $22^\circ\text{C} - 240^\circ\text{C} - 22^\circ\text{C}$ by time differential perturbed angular correlation measurement. For the application of this technique $(\text{Pb}_{0.925}\text{-Ba}_{0.075})\text{ZrO}_3$ was doped with small amounts of radioactive Hf^{181} . According to crystal structure studies this compound exhibits phase transitions at 175°C (antiferroelectric \rightarrow ferroelectric) and at $\sim 250^\circ\text{C}$ (ferroelectric \rightarrow paraelectric); it exhibits too a large temperature hysteresis at the lower transition⁽¹⁾. We were able to show that the electric field gradient (EFG) exhibits a sharp discontinuity at approximately 170°C , corresponding to the first phase transition, and slightly sharp discontinuity at approximately 200°C , corresponding to the second phase transition. In the cubic phase a remaining EFG is observed, which is probably caused by lattice imperfections in the source. We were not able to show any variation of the EFG following the hysteresis loop.

The measured EFG and the measured asymmetry coefficient of the EFG were compared with the result of a lattice sum calculation. As until now there is no any study of the variation of the cell parameters of $(\text{Pb}_{0.925}\text{-Ba}_{0.075})\text{ZrO}_3$, we established a criterium of atomic displacements based on the atomic displacements that occur in Pb ZrO_3 .

I. INTRODUCTION

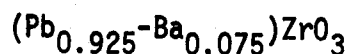
$(\text{Pb}_{0.925} - \text{Ba}_{0.075})\text{ZrO}_3$ is a compound with a perovskite-type structure. The perovskites show a tendency toward the formation of ferroelectric and antiferroelectric phases. In utilising various techniques such as dielectric constant measurements⁽¹⁾, neutron and X-ray diffraction^(2,3), Mössbauer spectroscopy^(4,5,6) a lot of information was stored about the phases and phase transitions of perovskites. As a consequence, a considerable knowledge has been gathered about the structure, the dielectric properties, the band character and the lattice dynamics of ferro- and antiferroelectric phases in perovskites. This paper presents a study of the temperature dependence of the EFG in polycrystalline lead-barium zirconate $(\text{Pb}_{0.925} - \text{Ba}_{0.075})\text{ZrO}_3$ by the time differential PAC technique. As the EFG is a measure of the internal charge arrangement in the compound, its investigation contributes, possibly, to the understanding of the collective phenomena in ferro- and antiferroelectric substances.

Systematic studies of the EFG in ferro- and antiferroelectric compounds are in the references (4-9).

As there is not a convenient isotope of Zr for the utilisation in PAC, $(\text{Pb}_{0.925} - \text{Ba}_{0.075})\text{ZrO}_3$ was doped with extremely small amounts of Hf^{181} , an ideal nucleus for PAC according to its intermediate level life-time and isotope life-time. Hf is immediately below Zr in Mendeleev's table of chemical elements and they show a pronounced similarity in their chemical behaviour; consequently, it could be expected that the doping of $(\text{Pb}_{0.925} - \text{Ba}_{0.075})\text{ZrO}_3$ by small amounts of radioactive Hf does not change the properties of the compound, and that the Hf^{4+} ions substitute Zr ions

in regular sites of the $(\text{Pb}_{0.925}\text{-Ba}_{0.075})\text{ZrO}_3$ lattice.

II. PROPERTIES OF LEAD ZIRCONATE (PbZrO_3) AND LEAD BARIUM ZIRCONATE



Since lead barium zirconate can be considered as the result of the replacement of Pb by Ba in the PbZrO_3 , we shall shortly discuss the dielectric and crystallographic properties of these compounds. The most characteristic features of PbZrO_3 , obtained by the study of a single crystal, are as follows⁽⁹⁾:

a) PbZrO_3 belongs to the perovskite family, and has two phases with different lattice structures. Below 230°C the unit cell is pseudotetragonal with $c/a < 1$; above this temperature it is cubic.

b) In the tetragonal phase the dielectric constant increases with temperature to reach a maximum at the Curie-temperature of $T_c = 230^\circ\text{C}$. In the cubic phase the compound is paraelectric and the dielectric constant decreases with $1/(T-T_c)$.

c) On application of external electric fields up to $30\text{kv}/\text{cm}$ no hysteresis loop is observed. At higher fields the compound changes from the anti-to a ferroelectric configuration, giving rise to a hysteresis.

d) An X-ray analysis of the tetragonal phase shows besides the main lines due to the perovskite structure some extra, so called super-lattice lines. A careful examination of these lines combined with additional neutron diffraction studies⁽³⁾ proves the antiferroelectricity of PbZrO_3 . The analysis shows that, with respect to the ideal perovskite structure, Pb atoms

suffer antiparallel shifts along the original cubic $[110]$ - direction, the oxygen atoms as well suffer antiparallel shifts within the (001) -plane and in addition unbalanced antiparallel shifts along the C - direction. The numerical values of these shifts are listed in table II of the ref.(3). These antiparallel displacements destroy the simple periodicity of the lattice structure. Periodicity is only regained by combining several unit cells to an orthorombic supercell. The superlattice created in this way gives rise to additional lines in the X-ray spectrum.

e) The variation of the cell parameters with the temperature is given in ref. (10). In respect to $(\text{Pb}_{0.925}\text{-Ba}_{0.075})\text{ZrO}_3$, it has been studied as ceramic by G. Shirane⁽¹⁾. It is of particular interest because, though neither of the end members Pb ZrO_3 and Ba ZrO_3 is ferroelectric, yet an intermediate phase is ferroelectric. Its essential properties compare to those of Pb ZrO_3 in the following way:

a) $(\text{Pb}_{0.925}\text{-Ba}_{0.075})\text{ZrO}_3$ as well is a member of the perovskite family. There exist however, three phases with different crystal structures, as follows: phase I (up to 170°C) is pseudotetragonal and antiferroelectric; phase II (170°C - 205°C) is rhombohedral and ferroelectric, with $c/a = 1$; phase III (above 205°C) is cubic. The variation of the lattice parameters as a function of the temperature are not yet known.

b) The dielectric constant has a peak in the upper transition, which increases in height and decreases in temperature with increasing amounts of Ba. At the boundary of the intermediate phase, there is a small anomaly. The rhombohedral phase shows a dielectric hysteresis loop.

c) $(\text{Pb}_{0.925} - \text{Ba}_{0.075})\text{ZrO}_3$ shows a large temperature hysteresis, of about 20°C wide, at the lower transition.

d) The X-ray spectrum of the compound is similar to that of Pb ZrO_3 . No neutron diffraction studies have been performed for up to now.

III. EXPERIMENTAL

The angular correlation of two successive γ -rays of a nuclear cascade may be perturbed when a coupling is established between the momenta of the intermediate nuclear state and extranuclear electromagnetic fields. Consequently the correlation will change in the time interval elapsed between the emission of the first and second γ -rays. In the angular correlation function this is taken into account by the perturbation factor $G_{kk}(t)$:

$$W(\theta, t) = 1 + A_2 G_{22}(t) P_2(\cos \theta) + A_4 G_{44}(t) P_4(\cos \theta) \quad (1)$$

All the physical information is contained in the $G_{kk}(t)$ function and most of the theoretical work had to deal with the derivation of appropriate formulae of $G_{kk}(t)$ for each type of interaction. Theoretical expressions for all kinds of static interactions are given by Steffen and Frauenfelder⁽¹⁾. Here we are concerned with static electric quadrupole interactions oriented randomly in space, acting on a nuclear level with spin $I = 5/2$. For this case the perturbation factor can be written as:

$$G_{kk}(t) = G_{k0} + \sum_{n=1}^3 \sigma_{kn} \cos(w_n t) \quad (2)$$

The σ_{k0} and σ_{kn} are given by Alder et al⁽¹²⁾, and Abragam and Pound⁽¹³⁾ for an axial field. The frequencies ω_n , in this expression, are the frequencies of the transition between the three hyperfine levels into which a state with $I = 5/2$ is split by an electric quadrupole field. These frequencies depend on two quantities characteristic for the interaction: an asymmetry parameter and a quadrupole frequency.

The EFG at the nucleus is described by the V_{ij} symmetrical tensor, which has six components. In the orthogonal (principal axis) system, this symmetrical tensor may be reduced to its diagonal form, that is to say, the number of components is reduced to V_{xx} , V_{yy} , V_{zz} . Since these components must obey Laplace's equation, $\nabla^2 V = 0$, only two of them are independent. Usually, the principal axes are chosen such that:

$$|V_{xx}| \leq |V_{yy}| \leq |V_{zz}| \quad (3)$$

The parameter η , mentioned above, is a measure of the asymmetry of the EFG - tensor, which interacts with the nuclear quadrupole moment and is defined by:

$$\eta = \frac{V_{xx} - V_{yy}}{V_{zz}} \quad (4)$$

From Laplace's equation and from equation (4), it follows that V_{xx} and V_{yy} have the same sign and therefore $0 \leq \eta \leq 1$.

The nuclear quadrupole frequency, also mentioned above, is defined by:

$$\omega_Q = \left| \frac{QV_{zz} e}{4I(2I-1)h} \right| \quad (5)$$

where Q is the spectroscopic quadrupole moment of the intermediate level of the cascade, and I its spin.

The asymmetry parameter and the quadrupole frequency can be deduced from the transition frequencies ω_n . A detailed account of the procedure is given in ref. (14). So a measurement of the perturbation factor $G_{kk}(t)$, from which the transition frequencies are obtained, permits the determination of all components of the EFG tensor, supposed the quadrupole moment of the investigated level is known.

2. SOURCE PREPARATION

The 133 KeV- 482 KeV $\gamma\gamma$ cascade of the 45 day- isotope Hf^{181} , which decays to Ta^{181} , is one of the most favourable cases for time differential angular correlation measurements. The life-time of the 482 KeV level is $T_{1/2} \sim 11$ nsec, its spin $I = 5/2$, the A_2 - coefficient of the cascade $A_2 \sim -0,25$; so that the experimental situation is relatively easy to handle. The radioactivity is obtained by the reaction $\text{Hf}^{180}(n,\gamma)\text{Hf}^{181}$. For the preparation of the polycrystalline $(\text{Pb}_{0.925}\text{-Ba}_{0.075})\text{ZrO}_3$ we followed the method applied by Forker et al⁽⁹⁾: to a mixture of equimolar portions of reagents grade ZrO_2 , BaCO_3 and PbO radioactive HfO_2 was added. The amount of HfO_2 added was ~ 0.01 mol-%. The mixture was vigorously grinded in a mortar; then, it was calcinated, at 1050°C , during one and a half hour; after calcination PbO was added to the mixture to compensate the evaporated one; the powder was then pressed to a pellet and sintered, at 850°C , during approximately forty hours. The low temperature of sintering was to prevent the evaporation of PbO , as Forker et al⁽⁹⁾. already noticed. The specimen sintered in such a way was free of ZrO_2 contribution and showed a X-ray picture similar to that of the PbZrO_3 .

3. THE EQUIPMENT

The time-differential measurements were performed with a two detector angular correlation apparatus. The detectors were two 56-AVP photomultipliers coupled to NaI(Tl) scintillation crystals, with dimensions of 2" x 2" (482 KeV) and 2" x 1" (133 KeV). The equipment diagram is in fig. (2); the time amplitude converter (TAC) was constructed by Forker⁽⁹⁾ and the slow part was a commercially available ORTEC system. The time resolution obtained for the energies of the relevant cascade varied between 2.9 nsec and 3.1 nsec f.h.w.m. The source temperature was varied in the range 22°C - 240°C - 22°C; to do it, a heating system was designed which yielded stability of approximately $\pm 1^\circ\text{C}$ for the source temperature.

4. PAC MEASUREMENTS, DATA TREATMENT AND RESULTS

The perturbation of the angular correlation was observed at the temperatures quoted in the table I. Coincidence spectra were taken at the angles 90°C, 135°C and 180°C, and from the spectra the coefficients $A_2G_{22}(t)$ were determined. The figs.(2-A, B) show the results of measurements at 22°C and 160°C, respectively.

The time spectra obtained in this way show slightly oscillations (fig. 2-A); such a damping of the angular correlation pattern is frequently observed. For solid sources it can be attributed to lattice imperfections and impurities. These lead to distributions of the frequency w_n , which are sharply defined only in a perfect crystal. In case the frequency distribution have gaussian shape with relative width δ , the perturbation factor takes the form:

$$G_{kk}(t) = G_{k0} + \sum_{n=1}^3 \sigma_{kn} \exp(-1/2 w_n^2 \delta^2 t^2) \cos(w_n t) \quad (6)$$

For the determination of the frequencies w_n and the relative width δ of their distribution this expression has been fitted to the measured time spectra. The least square fits took into account the finite time response of the equipment by numerical convolution of equation⁽⁶⁾ with the time resolution curve which had a width between 2.9 nsec- 3.1 nsec at half-maximum height. The solid lines in figs. (2-A, B) represent the result of the least square fits. From the fits the frequencies w_n and the widths of their distributions were deduced⁽¹⁴⁾. From the experimentally determined w_n the assymetry parameter η , the quadrupole frequency w_Q and the maximal component V_{zz} of EFG were calculated. Their values are in table I, for all the measured temperatures. Fig. (4) shows the temperature dependence of the EFG, obtained experimentally.

IV. DISCUSSION

According to the phase (fig. 5) and the thermal linear expansion (fig. 1) diagrams for the mixture $(Pb_{0.925} - Ba_{0.075})ZrO_3$ we could wait variations for the EFG, η parameters and quadrupolar frequency interactions values in the phase transition temperatures, with change of crystalline structure, and a hysteresis loop, with approximately 25°C wide for the EFG and the quadrupolar interaction frequency values at the lower transition. Our results show that (table I):

- a) The EFG value at 160°C is approximately 60% lower than at 22°C; as the η value dropped from 0.8, at 22°C, to about 0.4, at 160°C, the phase transition antiferroelectric (pseudotetragonal) \rightarrow ferroelectric (rhombohedral) must have occurred. The displacement of the transition point (170°C \rightarrow 160°C) can be due to the fact that we are not dealing with a perfect but

a real crystal with a certain amount of lattice irregularities or/and by the possibility that the percentage of Ba in the mixture is not exactly 7.5%. The decrease of the EFG value when we drop the temperature from 22°C to 160°C is most probably due to the temperature variation of the lattice parameters and the sudden change of the cell's parameters dimensions at the phase transition temperature. How the lattice parameters of $(\text{Pb}_{0.925} - \text{Ba}_{0.075})\text{ZrO}_3$ depend on temperature has not yet been studied; therefore, a direct comparison between the variation of the lattice parameters and the EFG values is not possible at present.

b) The EFG value decreases with the increasing of temperature; at 240°C, which is about 40°C above the cubic phase temperature, the EFG value is 15% of it's value at 22°C. Also the η coefficient decreases to values around zero. The phase transition which occurs at 205°C dont appear so sharply; but the η coefficient values, around zero, are a strong evidence that the actual phase is cubic. The non vanishing of the values in the cubic phase is due, again, to the fact that we are not dealing with a perfect but a real crystal, with a certain amount of lattice irregularities. Such imperfections will destroy the cubic simmetry at some lattice sites and thus will produce a small remaining interaction in the cubic phase, as we found it.

c) decreasing the temperature, after reaching 240°C, we notice that:

1 - the EFG and the η coefficient maintain, until 80°C - 100°C, the same values they had at 160°C;

2 - the frequency distribution begins to show, at temperature $\leq 100^{\circ}\text{C}$, values which are higher than 15%;

3 - the EFG value measured at 22°C , after the decreasing of the temperature, don't coincide with the EFG value found in the first measurement at the same temperature.

These last three items can be due to the fact that the original lattice symmetry is going to be destroyed, probably by the continuous heating of the material during the measurements. But according to the results obtained by Forker et al⁽⁹⁾ for the Pb ZrO_3 , it seems very improbable that this compound would be gradually destroyed by continuous heating. It can happen that the Ba ZrO_3 , sinterized at 850°C , is not sufficiently stable; so, it would begin to decompose in BaO and ZrO_2 , with a consequent change of the lattice original symmetry. The sintering temperature of Ba ZrO_3 , around $1,250^{\circ}\text{C}$ ⁽¹⁵⁾, seems to support such argument. As a matter of fact the X-ray picture of the material, taken after all measurements, showed ZrO_2 traces.

The exact atomic coordinates of $(\text{Pb}_{0.925} - \text{Ba}_{0.075})\text{ZrO}_3$ are not known. A lattice sum calculation was performed with the atomic positions in PbZrO_3 , as given in table II of ref.(3), modified by the following criterium: $(\text{Pb}_{0.925} - \text{Ba}_{0.075})\text{ZrO}_3$ mixture has a cubic structure; each Ba which substitutes one Pb in the $(1/2, 1/2, 0)$ position of Pb ZrO_3 will influence the other two Pb. As there will be six Pb atoms around each Ba atom, at an approximate distance of $4.1\overset{\circ}{\text{A}}$, the original displacement of each Pb, about $(\pm 0.088; \pm 0.0080; 0.0)$, will decrease in 33%, reaching the new values: $(\pm 0.058; \pm 0.0053; 0.0)$. According to this criterium, we obtained the presumible atomic displacements (table II).

The calculation yielded for the maximum component V_{zz} at 22°C , a value of $10.73 \times 10^{17}\text{V}/\text{cm}^2$, where the Sternheimer correction $(1-\gamma_{\infty})=62.2$ for Ta^{5+} has already been taken into account⁽¹⁶⁾. This value agrees within $\sim 75\%$ with the experimental result. A better agreement can not be expected, since dipolar and covalent contributions to the EFG have not been taken into account. Another source of error can be due to the criterium we used for the atomic displacements. The agreement is much better for the assymetry parameter η . The calculated value of 0.865 agrees within $\sim 90\%$ with the experimental value at room temperature (table I). This good agreement, as the assymetry parameter depends mainly of the symmetry of the lattice, can testify that our criterium of atomic displacements is not very far from the truth.

ACKNOWLEDGMENT

The authors are indebted to Dr. Augusto Baptista, from the Crystallographic Section of the Nuclear Engineering Institute of the National Nuclear Energy Commission for his helpful support by taking the X-ray pictures of the sample used in the measurements, and to Drs. Eder Suchinshy and Sergio Majdalani, from the Metallurgical Section of the same Institute, for their helpful support during the preparations of the samples. We are also indebted to the National Atomic Energy Commission and to the National Research Council of Brazil for financial support to this work.

TABLE I

ELECTRIC QUADRUPOLE INTERACTIONS MEASUREMENTS IN THE $(\text{Pb}_{0.925}\text{-Ba}_{0.075})\text{ZrO}_3$

T (°C)	ω (Mc/SEC)	η	ω_Q (Mc/SEG)	V_{ZZ} (10^{17}V/cm^2)	δ (%)
22(± 1)	612,0 ± 14,0	0,73 ± 0,05	69,7 ± 3,1	7,25 ± 0,43	5,4 ± 0,7
160(± 2)†	189,0 ± 8,5	0,375 ± 0,075	27,5 ± 1,9	2,86 ± 0,24	5,6 ± 1,1
180(± 3)†	123,1 ± 7,0	0,375 ± 0,090	17,9 ± 1,6	1,86 ± 0,18	5,03 ± 3,78
195(± 3)†	97,4 ± 7,2	0,0 ± 0,1	16,4 ± 2,0	1,71 ± 0,21	7,6 ± 5,5
205(± 3)†	91,7 ± 6,8	0,13 ± 0,20	14,3 ± 1,4	1,49 ± 0,15	5,0 ± 4,3
240(± 2)†	69,7 ± 17,0	0,00 ± 0,40	10,8 ± 1,9	1,12 ± 0,20	4,56 ± 19,5
140(± 2)†	185,5 ± 9,4	0,48 ± 0,10	25,5 ± 2,1	2,65 ± 0,22	10,7 ± 1,0
120(± 1)†	224,9 ± 6,1	0,60 ± 0,07	28,1 ± 1,6	2,93 ± 0,18	10,0 ± 1,0
100(± 1)†	221,4 ± 12,8	0,46 ± 0,16	30,2 ± 3,5	3,13 ± 0,37	5,3 ± 2,4
80(± 1)†	296,4 ± 18,5	0,49 ± 0,15	39,6 ± 4,9	4,12 ± 0,52	16,8 ± 2,8
50(± 1)†	319,1 ± 21,4	0,43 ± 0,19	44,4 ± 5,8	4,62 ± 0,60	24,4 ± 16,0
22(± 1)†	428,4 ± 14,2	0,60 ± 0,08	53,6 ± 3,9	5,58 ± 0,41	12,7 ± 2,5
160(± 2)†	157,4 ± 13,4	0,42 ± 0,15	21,5 ± 2,3	2,24 ± 0,24	10,0 ±
65(± 1)†	397,0 ± 18,1	0,56 ± 0,08	51,42 ± 5,57	5,35 ± 0,58	15,00 ± 3,6
140(± 1)†	187,14 ± 9,0	0,44 ± 0,10	26,14 ± 1,8	2,72 ± 0,17	14,34 ± 1,6

TABLE II
 ATOMIC DISPLACEMENT (IN FRACTION OF CELL EDGE)

	DISPLACEMENT IN THE PbZrO_3	DISPLACEMENT IN THE MIXTURE
Pb	$\pm 0,088$; $\pm 0,0080$; $0,00$	$\pm 0,058$; $\pm 0,0053$; $0,00$
Z _r	$\pm 0,014$; $\pm 0,0040$; $0,00$	$\pm 0,009$; $\pm 0,0025$; $0,00$
O _I	$\pm 0,040$; $\pm 0,100$; $\pm 0,040$	$\pm 0,010$; $\pm 0,025$; $\pm 0,010$
O _{II}	$\pm 0,080$; $\pm 0,080$; $\pm 0,100$	$\pm 0,020$; $\pm 0,020$; $\pm 0,025$
O _{III} O _{IV}	$0,00$; $0,00$; $\pm 0,10$	$0,00$; $0,00$; $\pm 0,025$

TABLE III

EQI CALCULATED RESULTS FOR VARIOUS Ba CONCENTRATIONS

% Ba	V_{xx}	V_{yy}	V_{zz}	$V_{zz}/V_{zz}(0\%)$	η	$V_{zz} \times 62,2(10^{17}V/cm^2)$
0,0	0,02499	0,07873	- 0,1070	1,00	0,518	9,04
2,3	0,02456	0,07843	- 0,10291	0,9829	0,523	9,04
5,2	0,02580	0,07757	- 0,10334	0,9965	0,501	9,03
8,1	- 0,00806	- 0,11142	0,4950	1,1524	0,865	10,52
10,0	- 0,00788	- 0,11101	0,11889	1,1465	0,567	10,51
12,2	- 0,00803	- 0,11074	0,11877	1,1453	0,863	10,59
14,9	- 0,00723	- 0,11239	0,11962	1,1535	0,879	10,52
17,8	- 0,01709	- 0,02092	0,03802	0,3666	0,101	3,34
19,9	- 0,01505	- 0,02323	0,03832	0,3695	0,213	3,34
22,3	0,60629	0,02863	- 0,03491	0,3366	0,640	3,08
24,8	0,00735	0,02707	- 0,03440	0,3317	0,513	3,06
27,3	0,00516	0,02881	- 0,03394	0,3273	0,697	3,05
29,8	0,00436	0,02811	- 0,03247	0,3191	0,731	2,86
32,7	0,00454	0,03013	- 0,03463	0,3339	0,739	3,00
34,6	2,00388	0,03155	- 0,03539	0,3412	0,782	3,08

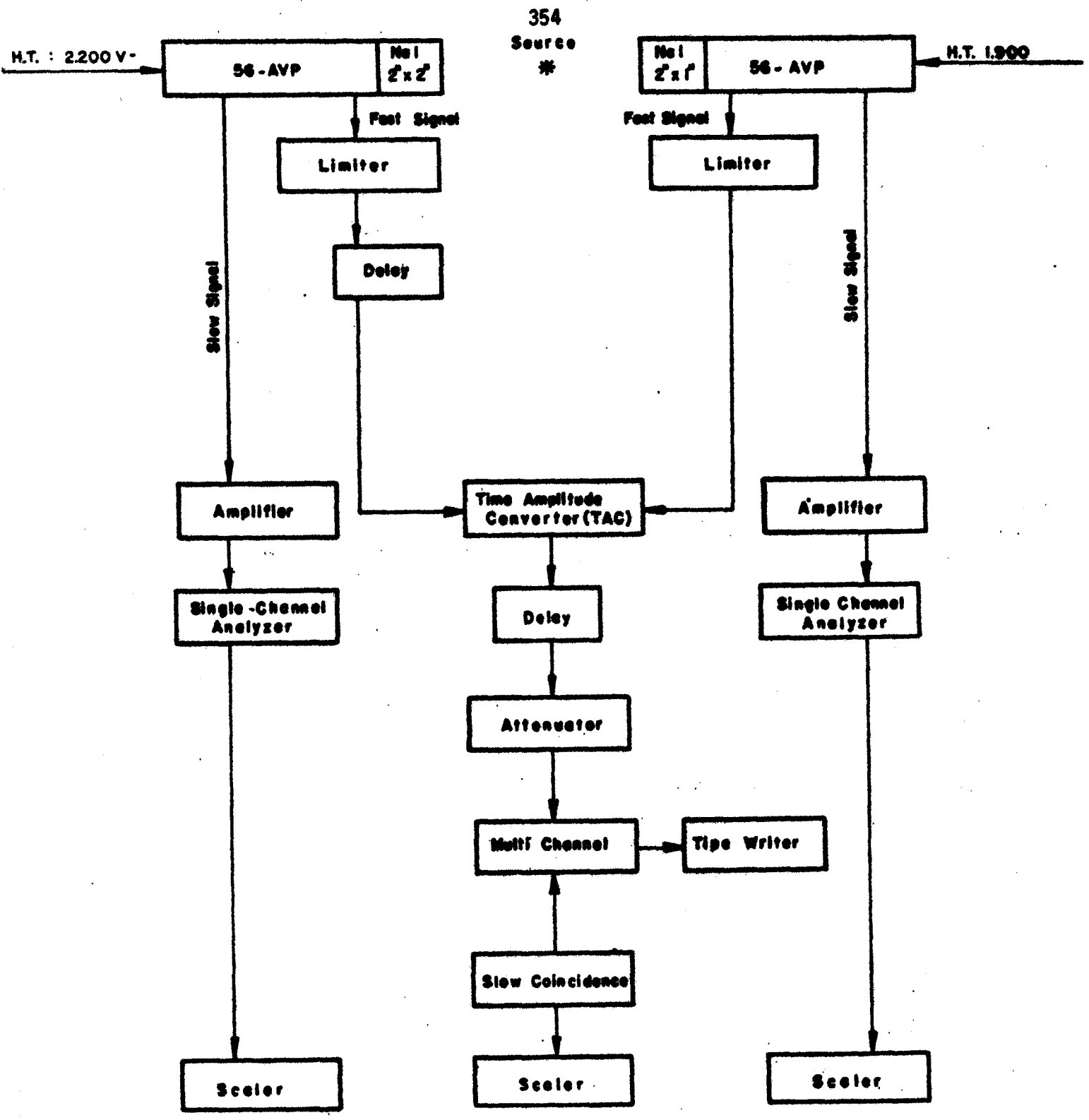


Fig 1 - EQUIPAMENT DIAGRAM

FIG. 2-A, T = 22°C

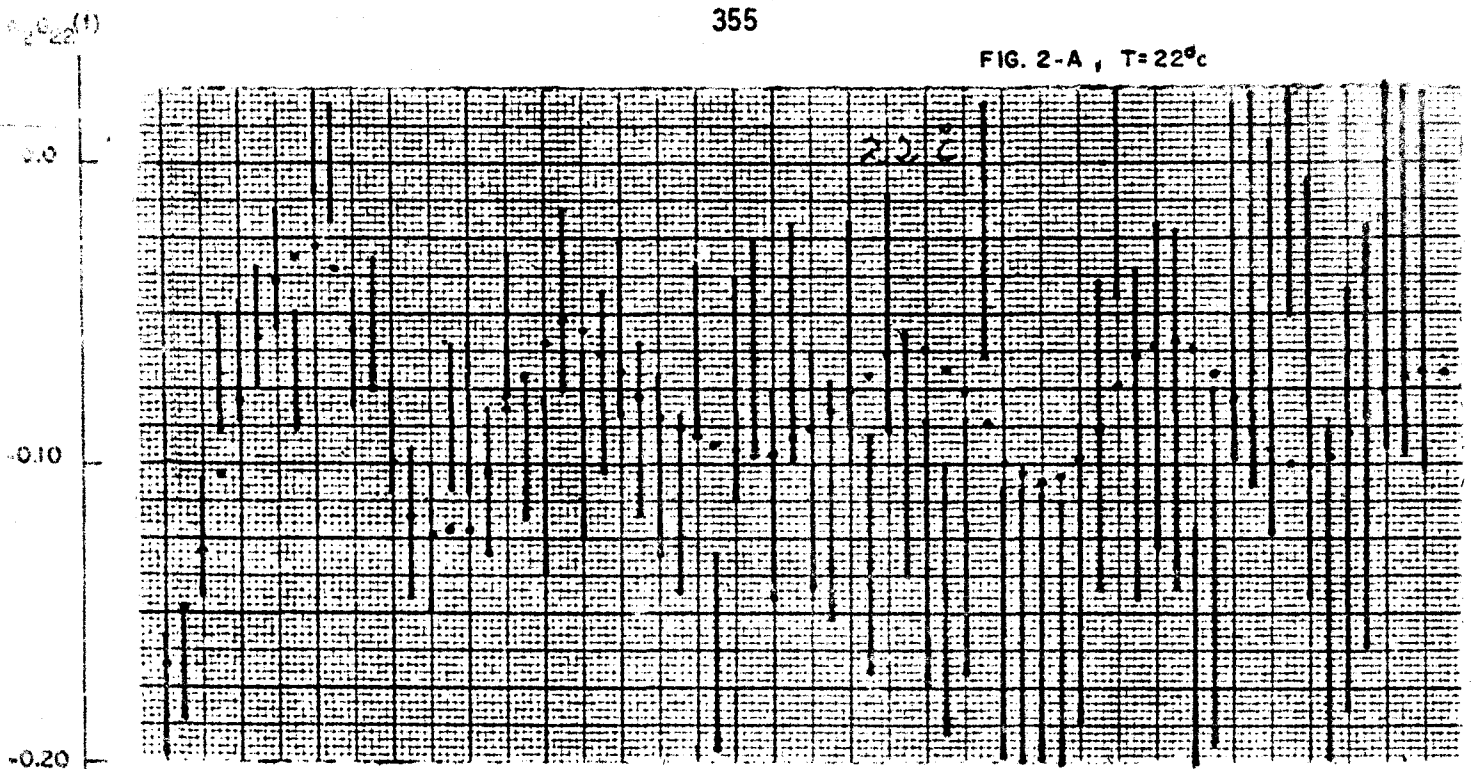


FIG. 2-B, T = 160°C

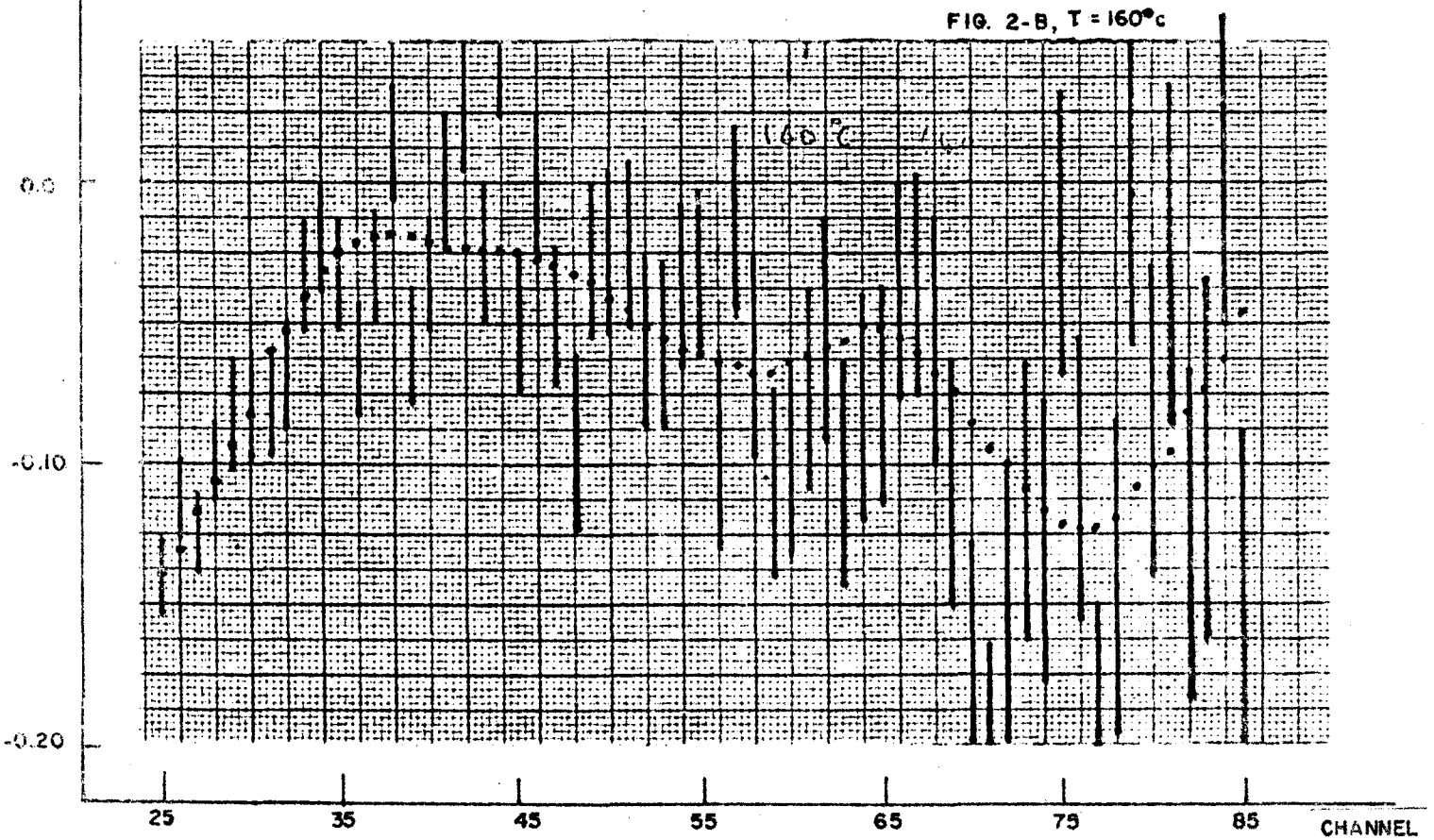


Fig. 2 (A,B) - PERTURBED ANGULAR CORRELATION OF Ta^{181} IN $(Pb.0.925 - Ba.0.075)ZrO_3$
 CALIBRATION: 0,6 nseg/channel